Supplementary Information

Enhancing Propane Dehydrogenation by Stabilizing Interfaces Systems on Porous Single-Crystalline Oxides

Xun Li,[a,b,c,d] Fangyuan Cheng *[a,b,c,d] and Kui Xie *[a,b,c,d,e]

[a] College of Physics and Energy, Fujian Normal University, Fuzhou 350117, China

[b] Key Laboratory of Design & Assembly of Functional Nanostructures, Fujian Institute of Research on the Structure of Matter, Chinese Academy of Sciences, Fuzhou, Fujian, 350002, China

[c] Fujian Science & Technology Innovation Laboratory for Optoelectronic Information of China, Fuzhou, Fujian, 350108, China

[d] Fujian College, University of Chinese Academy of Sciences, Fuzhou, Fujian 350108, China

[e] School of Mechanical Engineering, Shanghai Jiao Tong University, 800 Dongchuan Road, Shanghai, 200240, China

* Corresponding author: cfy@fjirsm.ac.cn (F. Cheng), xiekui@sjtu.edu.cn (K. Xie).

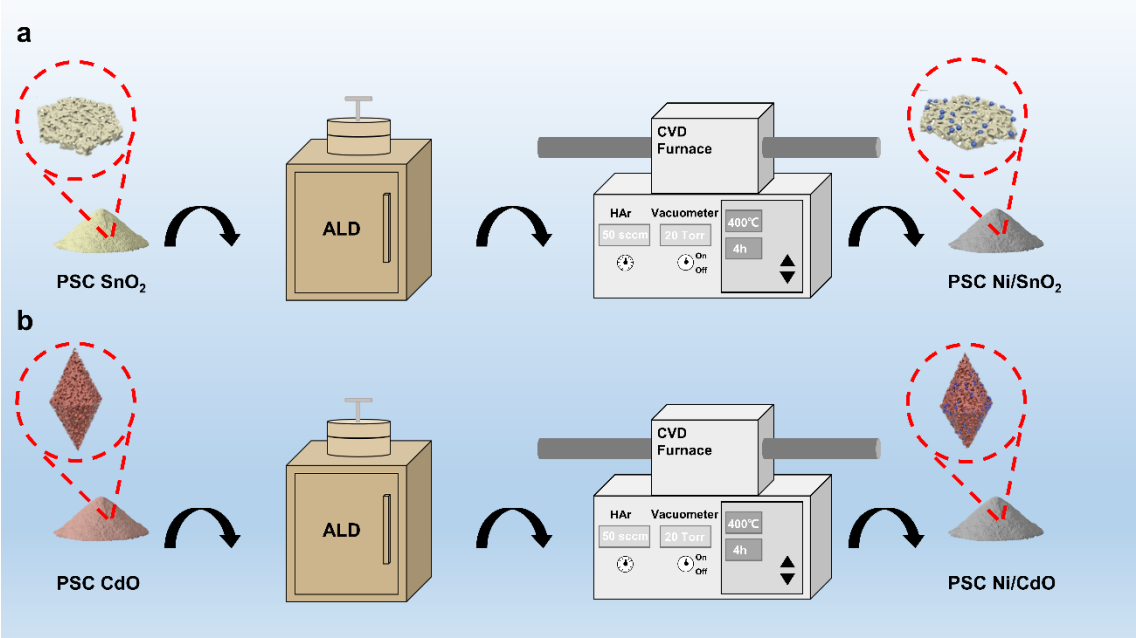

Fig. S1 Schematic diagrams of the (a) PSC Ni/SnO_2 and (b) PSC Ni/CdO preparation processes.

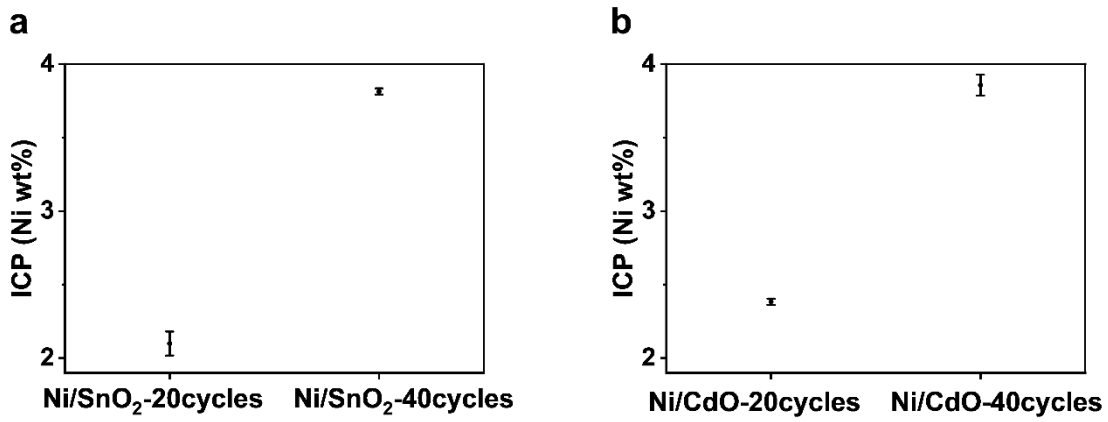

Fig. S2 ICP tests of (a) PSC Ni/SnO_2 and (b) PSC Ni/CdO with different loading levels of Ni NPs.

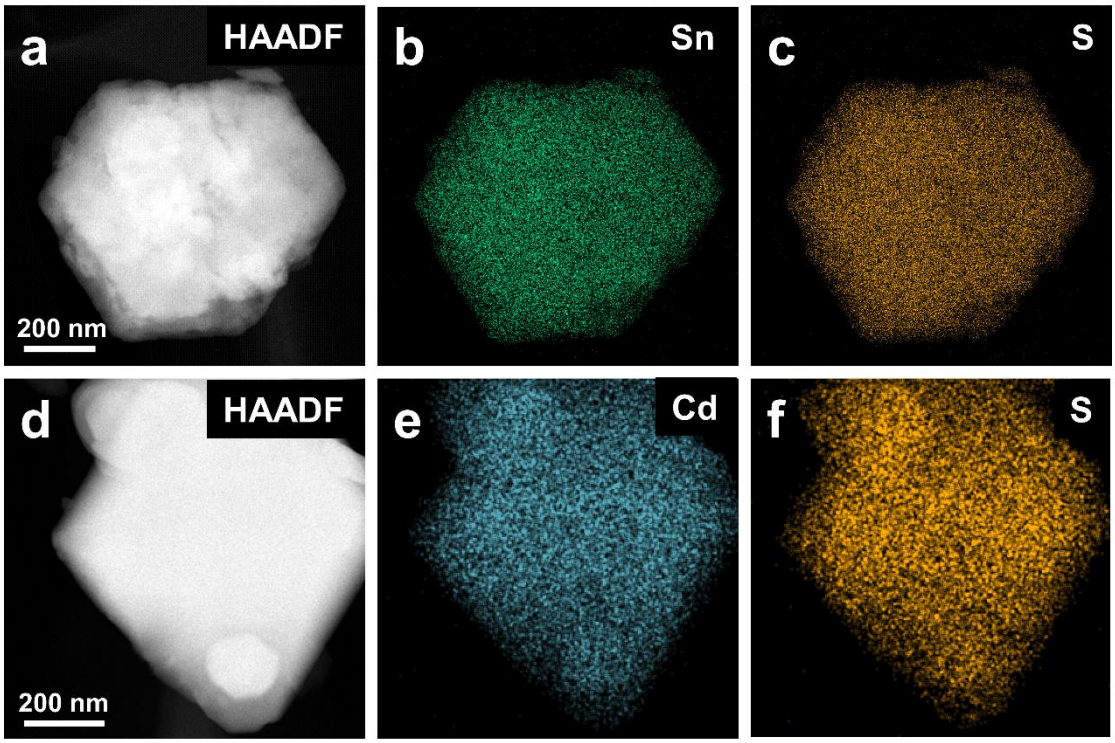

Fig. S3 HAADF and elemental mapping images of (a-c) SnS_2 and (d-f) CdS precursors.

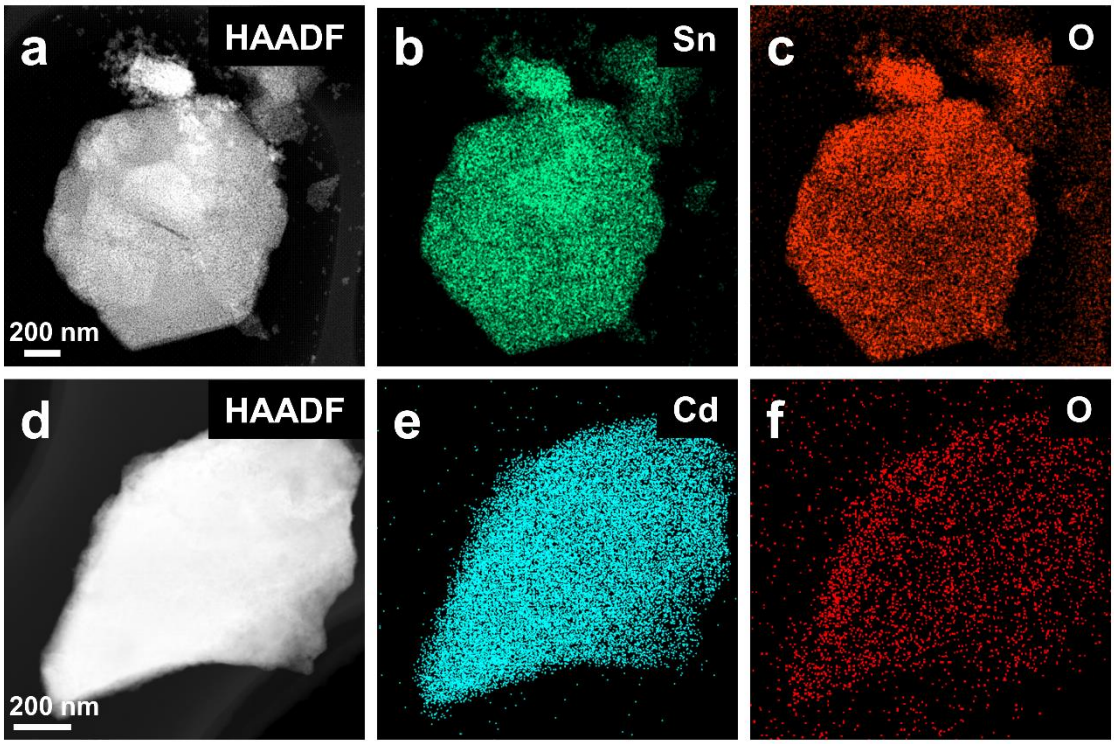

Fig. S4 HAADF and elemental mapping images of (a-c) PSC SnO_2 and (d-f) PSC CdO.

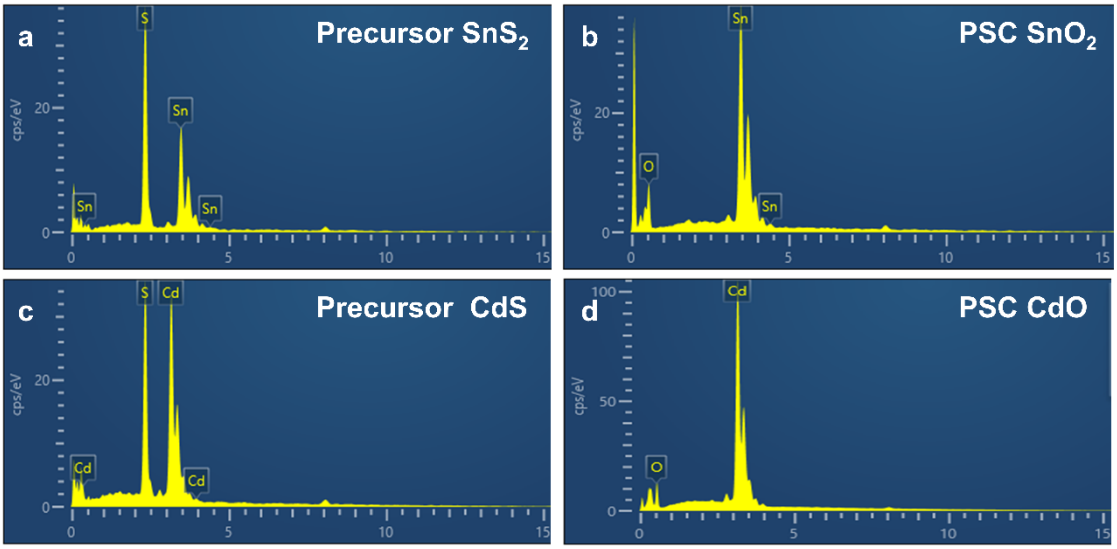

Fig. S5 EDS tests of (a) SnS_2 precursor, (b) PSC SnO_2, (c) CdS precursor and (d) PSC CdO.

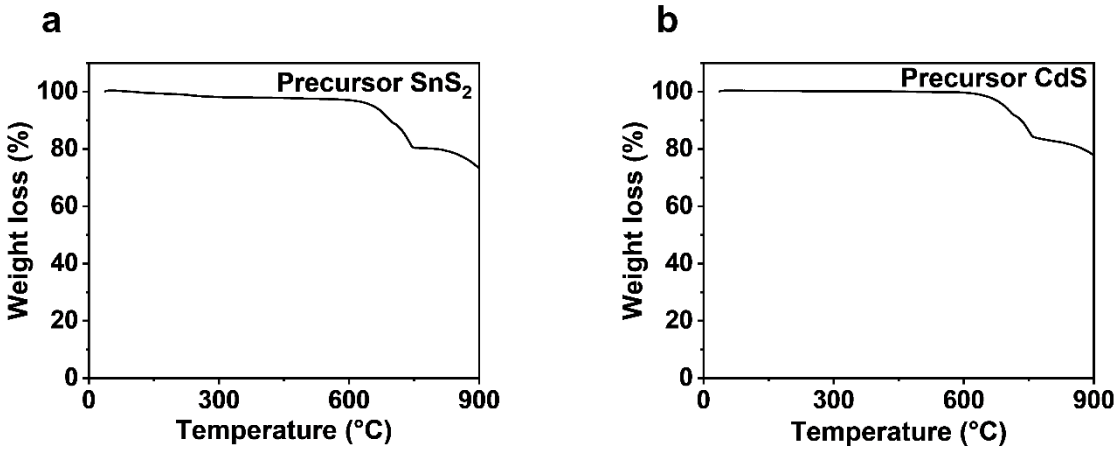

Fig. S6 TGA tests of (a) SnS_2 and (b) CdS precursors.

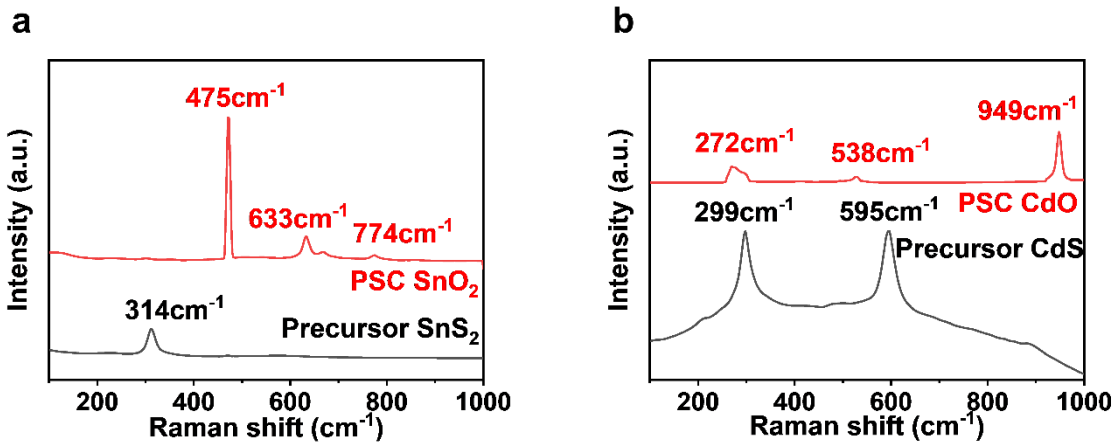

Fig. S7 (a, b) Raman spectra of SnS_2 precursor, PSC SnO_2, CdS precursor and PSC CdO.

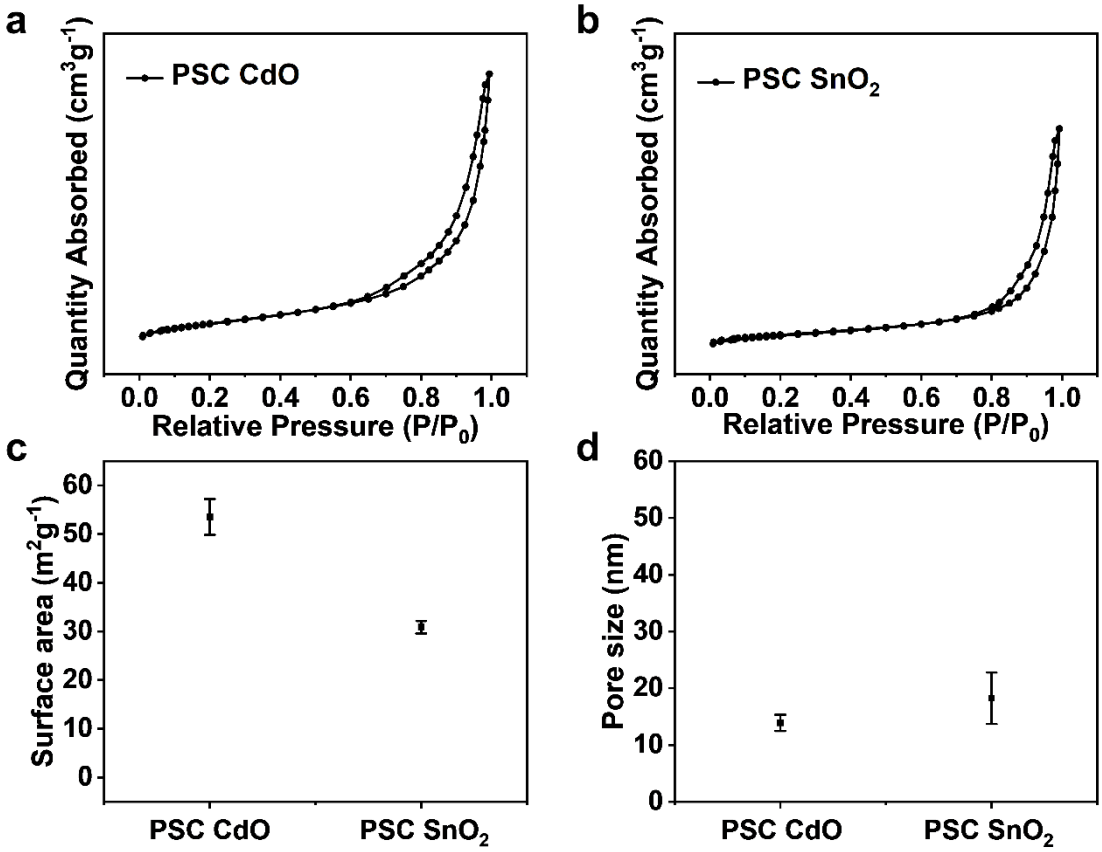

Fig. S8 N_2 adsorption and desorption diagrams of (a) PSC CdO and (b) PSC SnO_2. (c, d) Specific surface areas and average pore sizes of PSC CdO and PSC SnO_2.

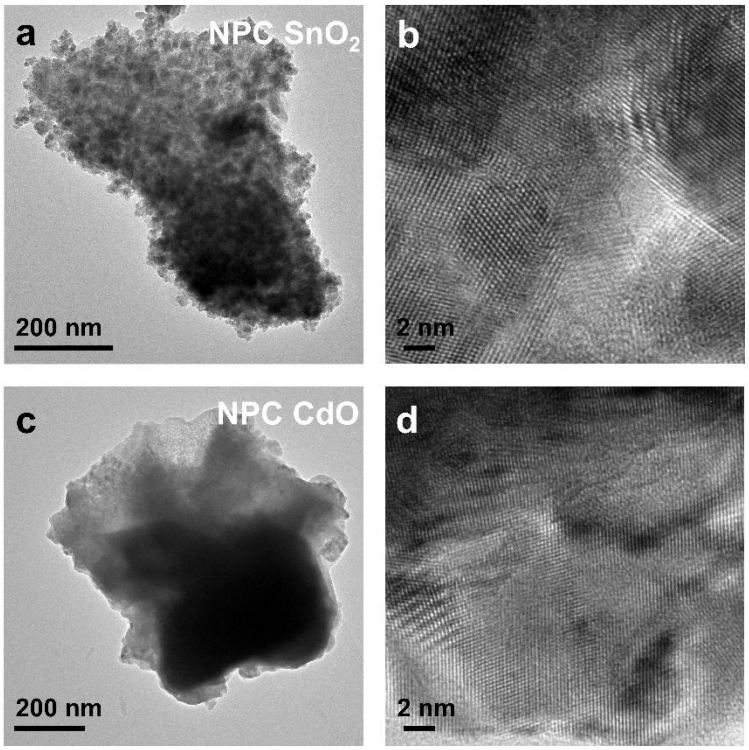

Fig. S9 (a, b) TEM image, HRTEM image of NPC SnO_2. (c, d) TEM image, HRTEM image of NPC CdO.

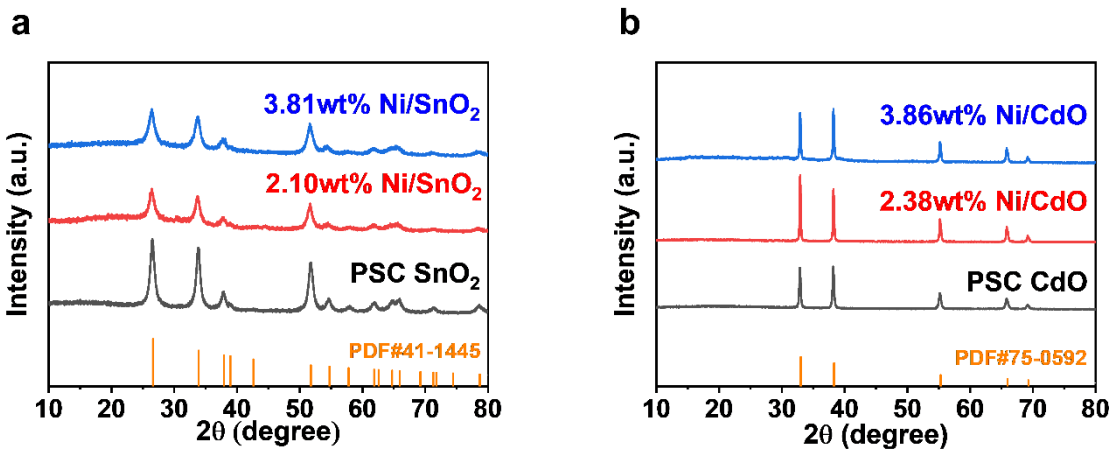

Fig. S10 XRD patterns of (a) PSC SnO_2 and (b) PSC CdO with different loading levels of Ni NPs.

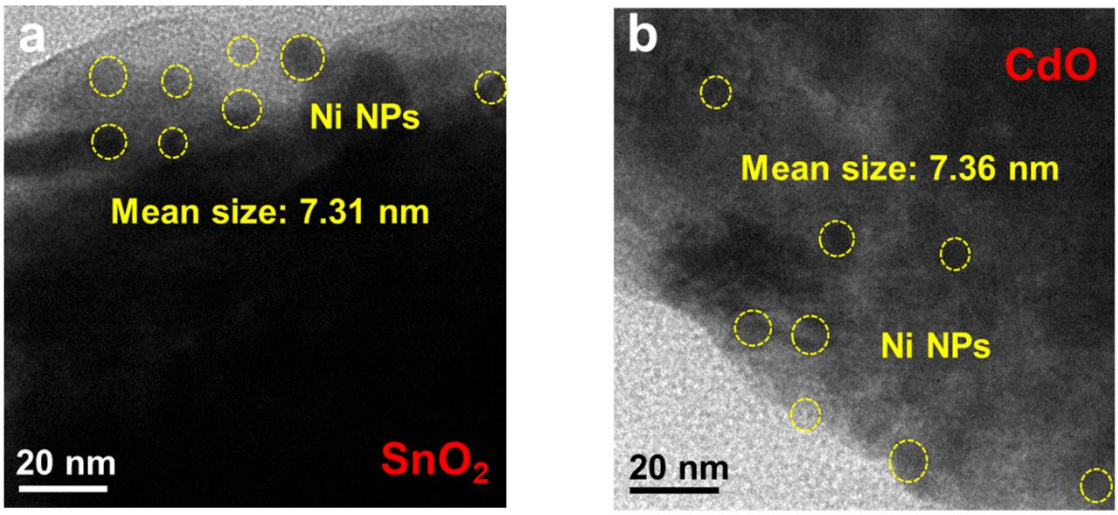

Fig. S11 HRTEM images of (a) PSC Ni/SnO_2 and (b) PSC Ni/CdO.

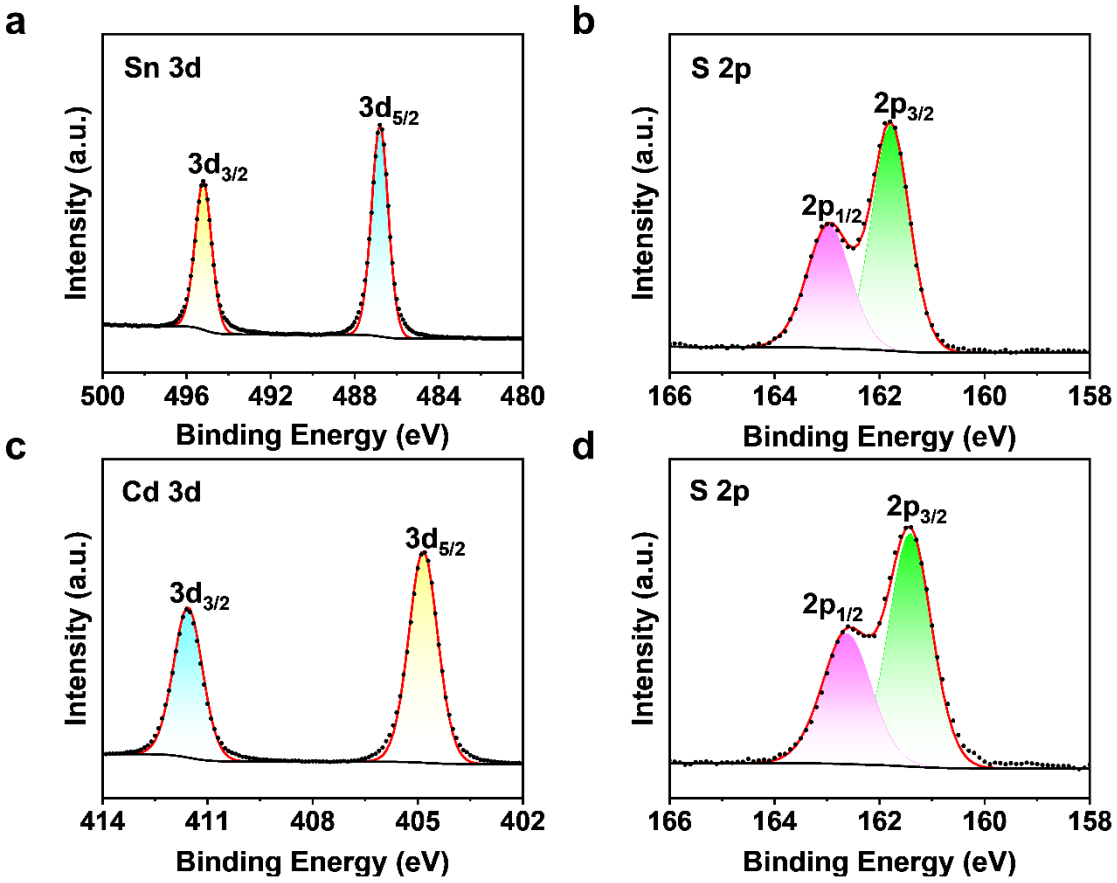

Fig. S12 XPS spectra of (a, b) SnS_2 and (c, d) CdS precursors.

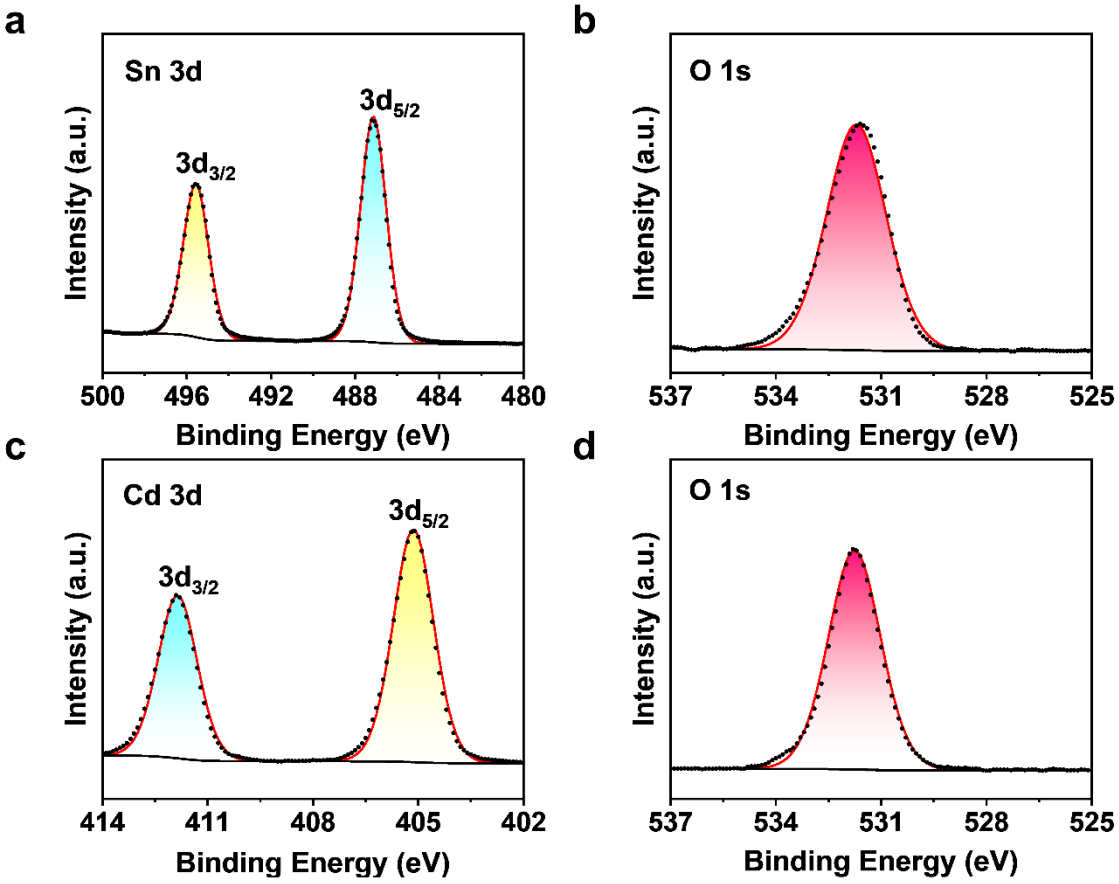

Fig. S13 XPS spectra of (a, b) PSC SnO_2 and (c, d) PSC CdO.

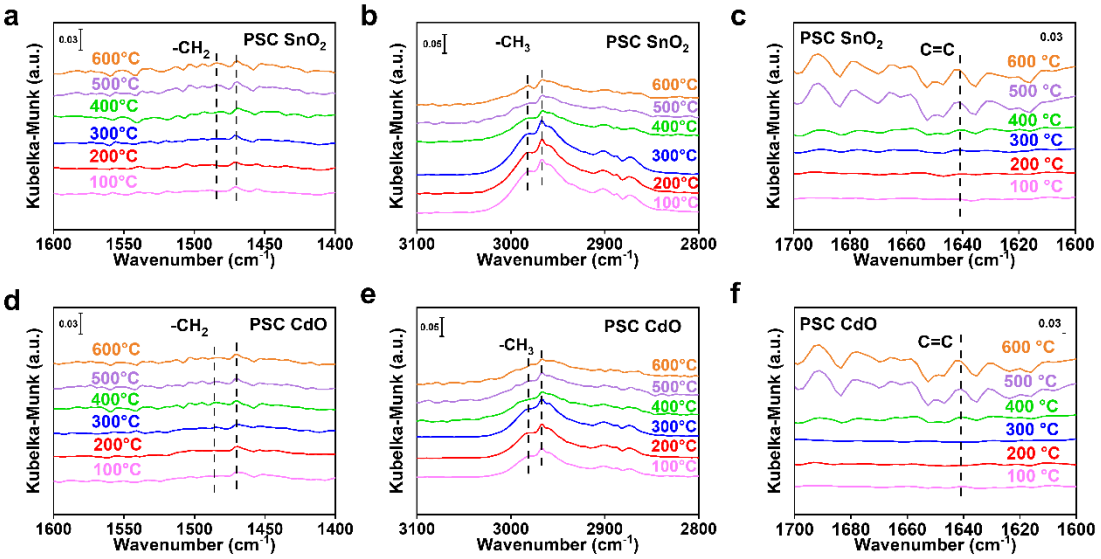

Fig. S14 *In situ* FTIR of (a-c) PSC SnO_2 and (d-f) PSC CdO in PDH reaction.

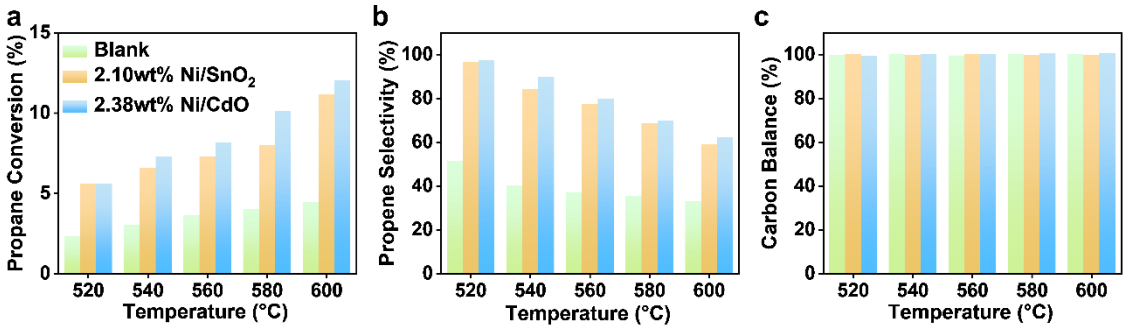

Fig. S15 (a) Propane conversion, (b) propylene selectivity and (c) carbon balance of blank control group, 2.10 wt% Ni/SnO_2 and 2.38 wt% Ni/CdO in PDH reaction. Reaction conditions: WHSV=3000 mL g_{cat}^{-1} h^{-1}.

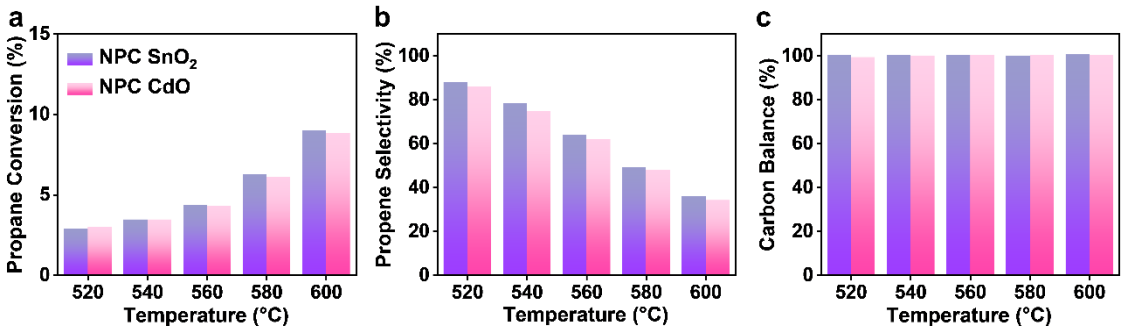

Fig. S16 (a) Propane conversion, (b) propylene selectivity and (c) carbon balance of NPC SnO_2 and NPC CdO in PDH reaction. Reaction conditions: WHSV=3000 mL g_{cat}^{-1} h^{-1}.

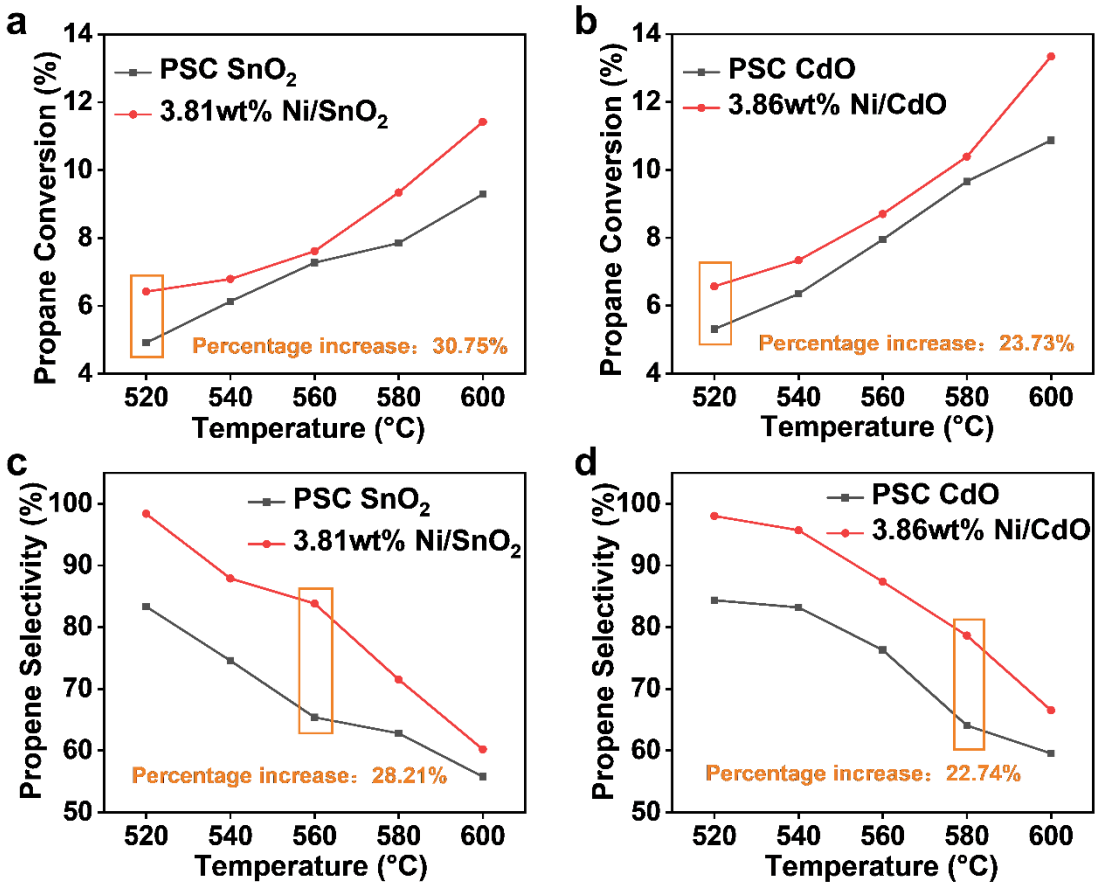

Fig. S17 (a, b) Ni/metal-oxide interfaces significantly enhances propane conversion in PDH reaction. (c, d) Ni/metal-oxide interfaces significantly enhances propylene selectivity in PDH reaction. Reaction conditions: WHSV=3000 mL g_{cat}^{-1} h^{-1}.

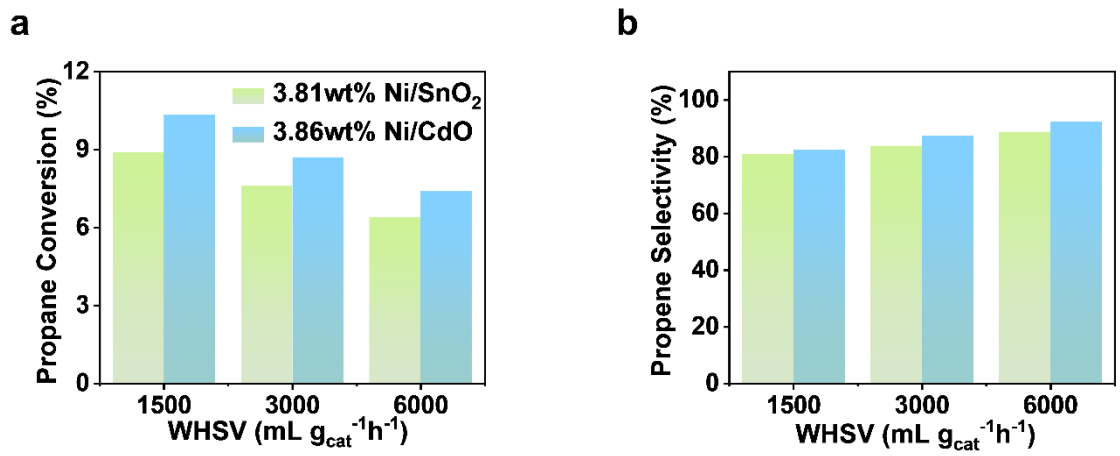

Fig. S18 (a) Propane conversion and (b) propylene selectivity of 3.81 wt% Ni/SnO_2 and 3.86 wt% Ni/CdO at 560 °C under different WHSVs in PDH reaction.

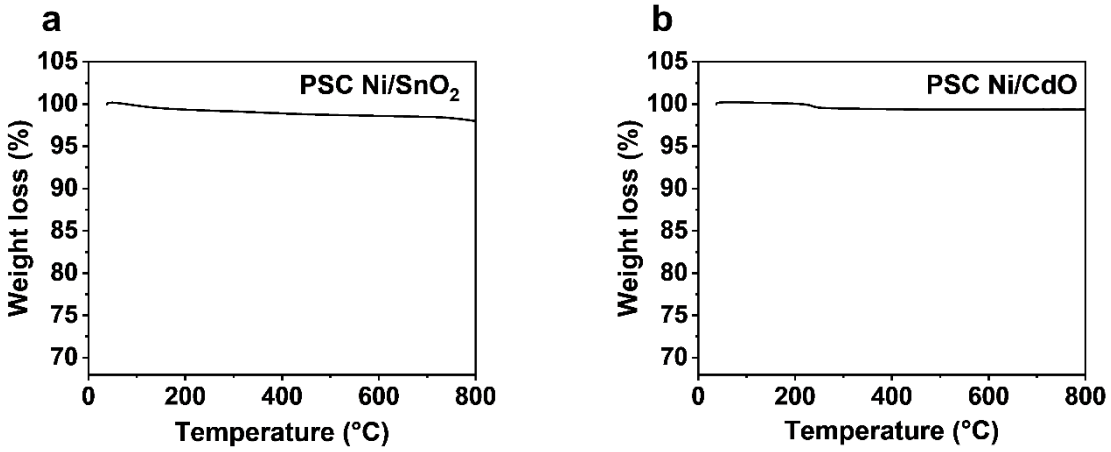

Fig. S19 TGA tests of (a) PSC Ni/SnO_2 and (b) PSC Ni/CdO after stability tests.

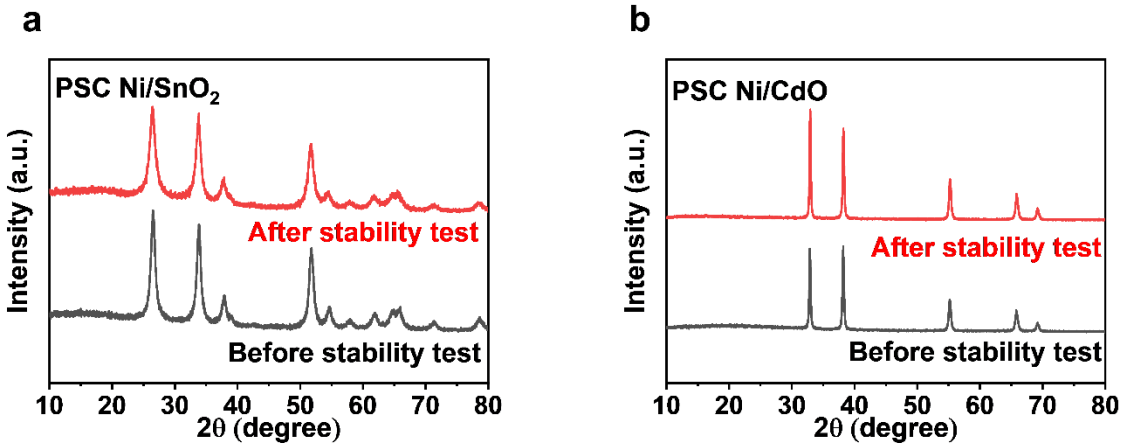

Fig. S20 XRD patterns of (a) PSC Ni/SnO_2 and (b) PSC Ni/CdO before and after stability tests.

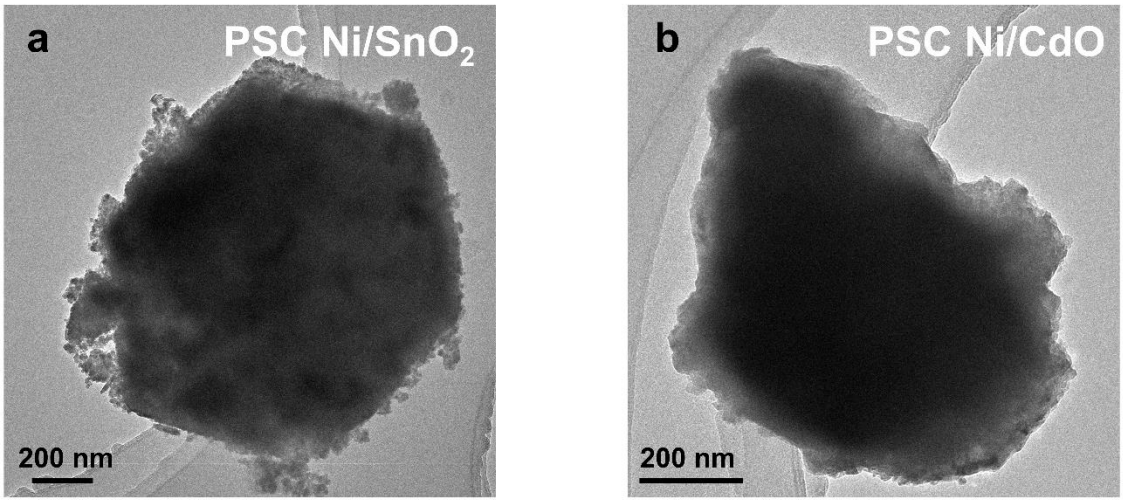

Fig. S21 TEM images of (a) PSC Ni/SnO_2 and (b) PSC Ni/CdO after stability tests.

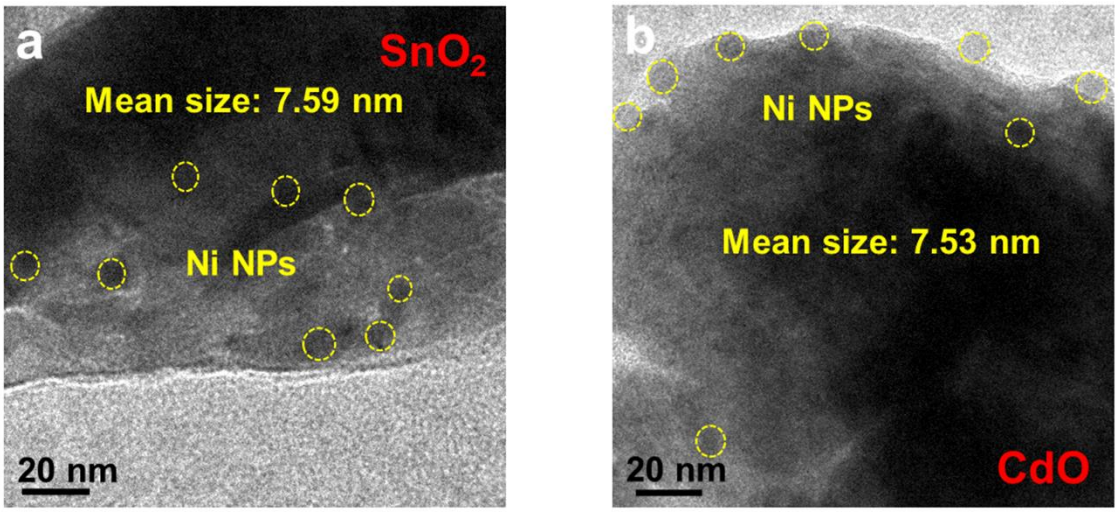

Fig. S22 HRTEM images of (a) PSC Ni/SnO_2 and (b) PSC Ni/CdO after stability tests.